Electronic Supplementary Material (ESI) for Journal of Materials Chemistry A.
This journal is © The Royal Society of Chemistry 2020

Topologically distributed one-dimensional TiO_2 nanofillers maximize the dielectric energy density in P(VDF-HFP) nanocomposite

Xiaoru Liu, Penghao Hu*, Jinyao Yu, Mingzhi Fan, Xumin Ji, Binzhou Sun, Yang Shen*

*Corresponding author

Email address: huph@ustb.edu.cn (P.H. Hu), shyang_mse@mail.tsinghua.edu.cn (Y. Shen)

Electronic supplementary information

The morphology of the TO nanorods arrays was determined by both the hydrothermal reaction time and reactant concentration, where the diameter and the height of the nanorods arrays simultaneously increase with time extension and/or concentration rising, as seen in Fig. S1. The representative samples of (a1), (b2) & (c3) were chosen as the nanofillers to fabricate TO-A/P(VDF-HFP) nanocomposite films.

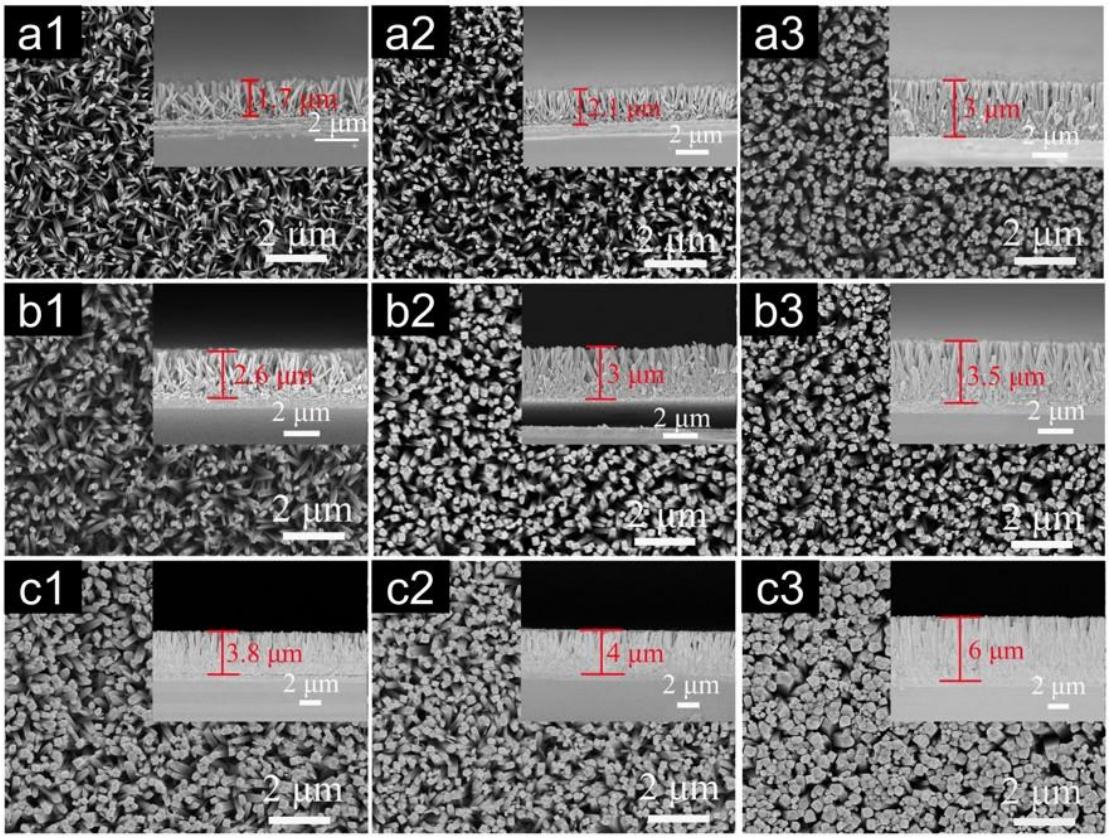

Fig. S1 Vertical view SEM images of the TO nanorods arrays prepared with different reactant concentrations and reaction times in hydrothermal method. (a1) 0.036 mol/L, 6 h; (a2) 0.042 mol/L, 6 h; (a3) 0.048 mol/L, 6 h; (b1) 0.036 mol/L, 8 h; (b2) 0.042

mol/L, 8 h, (b3) 0.048 mol/L, 8 h; (c1) 0.036 mol/L, 10 h, (c2) 0.042 mol/L, 10 h, (c3) 0.048 mol/L, 10 h.

Fig. S2 shows the cross-sectional morphology of the nanocomposite films named TO-A-1/P(VDF-HFP), TO-A-2/P(VDF-HFP) and TO-A-3/P(VDF-HFP) embedded with the representative TO-A samples as seen in (a1), (b2) & (c3) in Fig. S1, respectively. The composite films are dense and represent a distinct dividing line between the TO-A at the bottom side and the pristine P(VDF-HFP) at the top side.

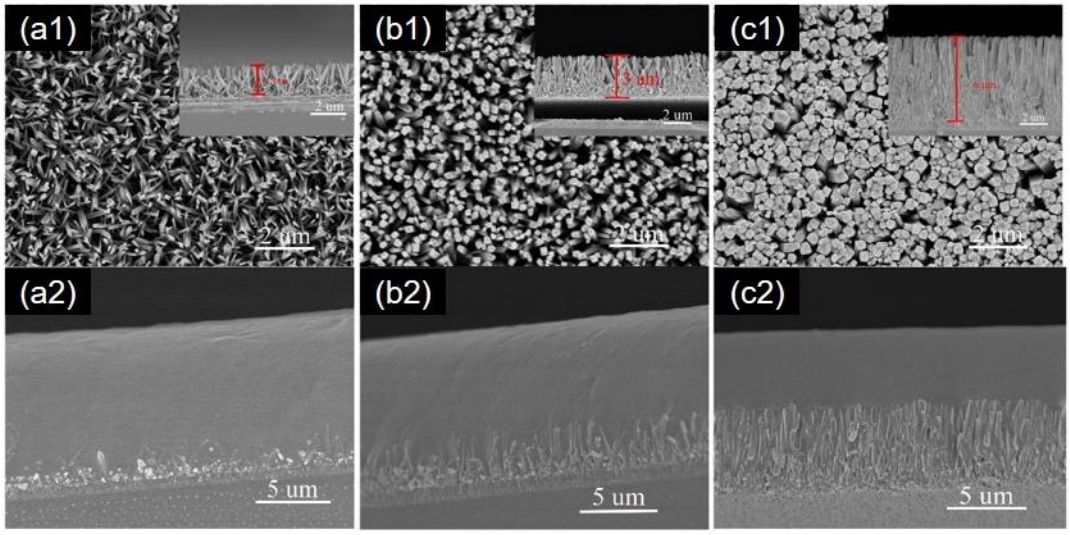

Fig. S2 SEM images of vertical view of the TO nanorod arrays (a1) 0.036 mol/L, 6 h; (b1) 0.042 mol/L, 8 h, (c1) 0.048 mol/L, 10 h, and the cross-sectional morphology of corresponding nanocomposites of (a2) TO-A-1/P(VDF-HFP), (b2) TO-A-2/P(VDF-HFP) and (c2) TO-A-3/P(VDF-HFP).

The top view of TO-F/P(VDF-HFP) nanocomposite films contained with 1~7 vol% TO-F are shown in Fig. S3. The TO nanofibers can be clearly observed in the matrix with uniform dispersion. With the solution casting process, all the nanofibers represent random and in-plane (or small angles) distribution in the matrix.

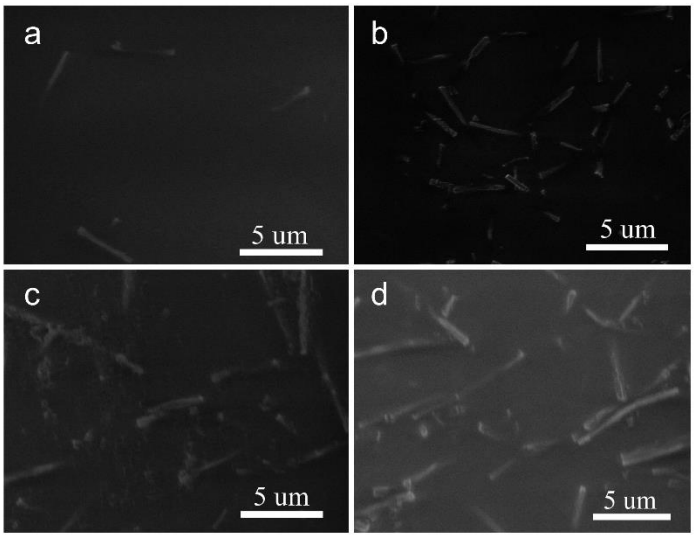

Fig. S3 SEM images of the surface appearance of TO-F/P(VDF-HFP) contained with different TO-F content: (a) 1 vol%, (b) 3 vol%, (c) 5 vol%, (d) 7 vol%.

As shown in Fig. S4(b) & S5(b), the breakdown strengths of the nanocomposite films were analyzed according to a two parameter Weibull distribution function [1,2]:

$$P(E) = 1 - \exp(-(E / E_b)\beta) \quad (1)$$

where P(E) is the cumulative probability of electric failure, E is experimental breakdown electric field, E_b is a scale parameter refers to the breakdown strength at the cumulative failure probability of 63.2% which is regarded as the breakdown strength of the measured sample, and β is the Weibull modulus associated with the linear regressive fit of the distribution.

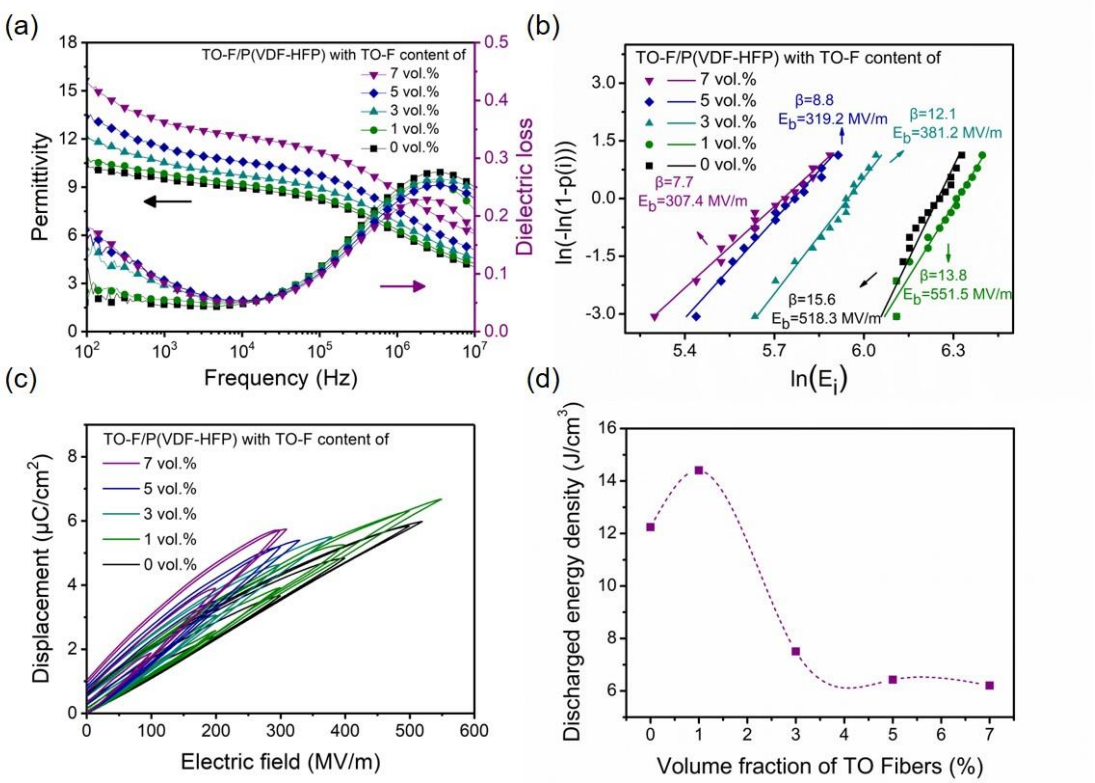

Fig. S4 (a) The dielectric permittivity and dielectric loss spectra versus frequency, (b) failure probability of dielectric breakdown deduced from Weibull distribution, (c) *D-E* loops and (d) the maximal discharged energy density of TO-F/P(VDF-HFP) nanocomposites contained with different TO-F.

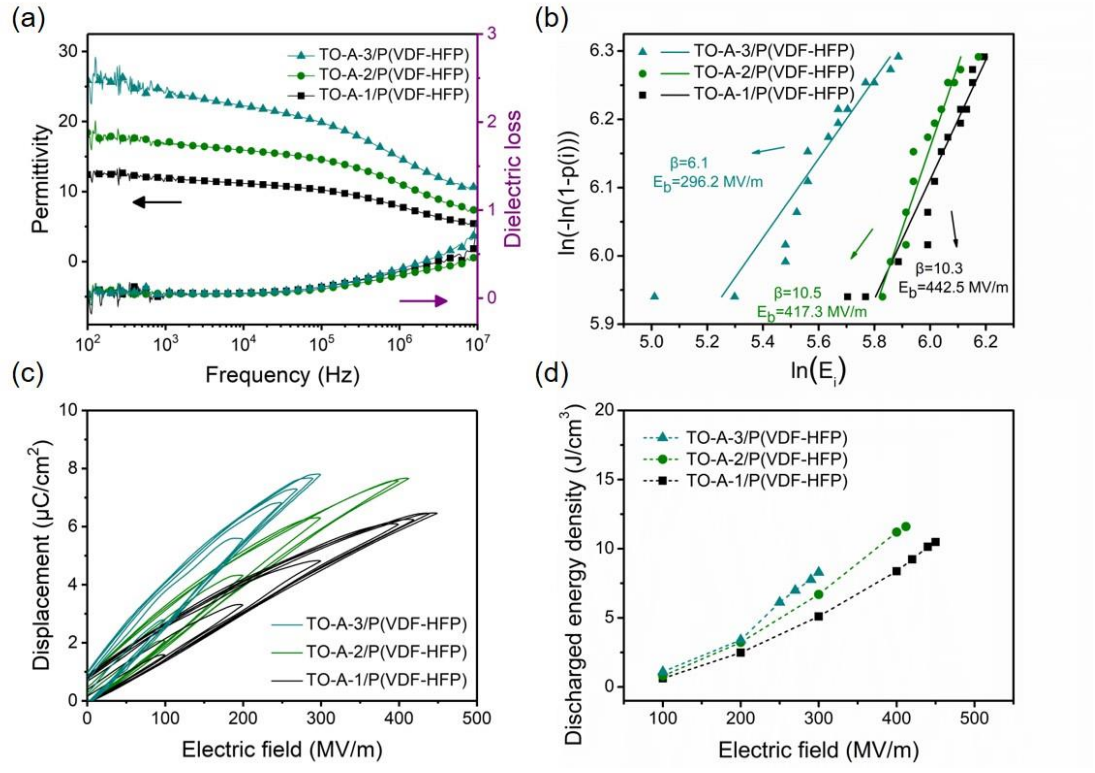

Fig. S5 (a) The dielectric permittivity and dielectric loss spectra versus frequency, (b) failure probability of dielectric breakdown deduced from Weibull distribution, (c) *D-E* loops and (d) the discharged energy density versus electric filed of the TO-A/P(VDF-HFP) nanocomposites.

Thermogravimetric curves of TO-A/P(VDF-HFP) and TO-A/TO-F/P(VDF-HFP) were exhibited in Fig. S6. The equivalent content of TO nanofillers contained in the nanocomposite was calculated from the residual weight. The TO-A in TO-A/P(VDF-HFP) is 6.629 vol%, and the sum of TO-A and TO-F in TO-A/TO-F/P(VDF-HFP) is 7.584 vol%.

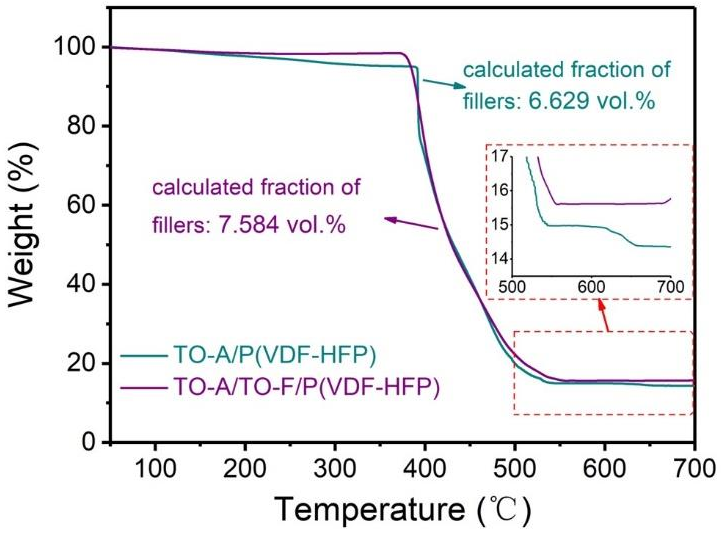

Fig. S6 TG curves of TO-A/P(VDF-HFP) and TO-A/TO-F/P(VDF-HFP).

Fig. S7 exhibits the failure probability data of the nanocomposite films, including pristine P(VDF-HFP), 1 vol% loading TO-F/P(VDF-HFP), the optimized TO-A/P(VDF-HFP) and TO-A/TO-F/P(VDF-HFP), in Weibull distribution. The breakdown strength and the Weibull modulus values are shown in the Figure.

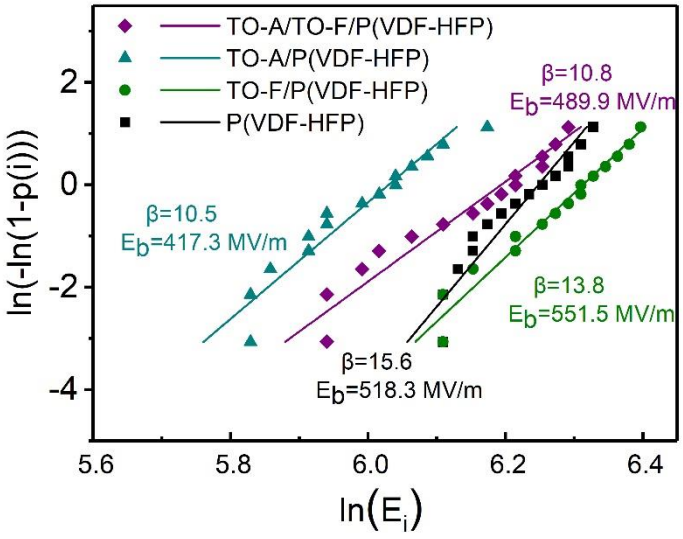

Fig. S7 Failure probability of dielectric breakdown of the nanocomposite films deduced from Weibull distribution.

To obtain the electric displacement, the Spectral Iterative Perturbation Method (SIPM) was employed to solve the electrostatic equilibrium equations for the TO-A/P(VDF-HFP) and TO-A/TO-F/P(VDF-HFP) nanocomposites. The charge density distribution $\rho(\mathrm{r})$ in the composite films can be attained from the overall polarization field $\mathbf{P}(\mathrm{r})$ according to Phase-field simulation model [3,4]:

$$\rho(\mathrm{r}) = -\nabla \cdot \mathrm{P}(\mathrm{r}) \tag{2}$$

where $\mathbf{P}(\mathrm{r})$ is the sum of the spontaneous polarization $\mathbf{P}^{\mathrm{s}}(\mathrm{r})$ and the induced polarization $\mathbf{P}^{\mathrm{E}}(\mathrm{r},\mathrm{E})$. $\mathbf{P}^{\mathrm{s}}(\mathrm{r})$ deduced from the permanent electric moment due to the intrinsic polar of dielectrics and ferroelectrics, while $\mathbf{P}^{\mathrm{E}}(\mathrm{r},\mathrm{E})$ is determined by the total electric field $\mathbf{E}(\mathrm{r})$ as follows:

$$\mathrm{P}^{\mathrm{E}}(\mathrm{r},\mathrm{E}) = \varepsilon_0 \chi(\mathrm{r})\,\mathrm{E}(\mathrm{r}) \tag{3}$$

where $\boldsymbol{\chi}(\mathrm{r})$ represents the dielectric susceptibility. The electric field distribution $\mathbf{E}(\mathrm{r})$ is obtained from the electrostatic equilibrium equation:

$$\nabla \cdot \mathrm{D}(\mathrm{r}) = \nabla \cdot (\varepsilon_0 \kappa(\mathrm{r})\,\mathrm{E}(\mathrm{r}) + \mathrm{P}^{\mathrm{S}}(\mathrm{r})) = 0 \tag{4}$$

with $\boldsymbol{\kappa}(\mathrm{r}) = \boldsymbol{\delta} + \boldsymbol{\chi}(\mathrm{r})$. For such a dielectric inhomogeneous composite, a spectral iterative

perturbation method was employed to solve equation (3) according to

$$\kappa_{ij}^{0}\frac{\partial^{2}\varphi(\mathrm{r})}{\partial x_{i}\partial x_{j}}=\frac{\partial}{\partial x_{i}}[\Delta\kappa_{ij}(\mathrm{r})E_{j}(\mathrm{r})]+\frac{1}{\varepsilon_{0}}\frac{\partial \mathrm{P}_{i}^{\mathrm{S}}(\mathrm{r})}{\partial x_{i}} \tag{5}$$

where φ(r) represents the local electric potential with $E_j(r) = -\nabla_j \boldsymbol{\varphi}(r)$. In addition, the position-dependent relative permittivity $\boldsymbol{\kappa}_{ij}(r)$ is written as a sum of homogeneous reference κ_{ij}^{0} and inhomogeneous perturbation $\Delta\kappa_{ij}(r)$ [5].

References

[1] V. Tomer, E. Manias, C.A. Randall, high field properties and energy storage in nanocomposite dielectrics of poly(vinylidene fluoride-hexafluoropropylene), J. Appl. Phys. 110 (2011) 044107.

[2] S.P. Fillery, H. Koerner, L. Drummy, E. Dunkerley, M.F. Durstock, D.F. Schmidt, R.A. Vaia, Nanolaminates: increasing dielectric breakdown strength of composites, ACS Appl. Mater. Interfaces 4 (2012) 1388-1396.

[3] J.J. Wang, X.Q. Ma, Q. Li, J. Britson, L.Q. Chen, Phase transitions and domain structures of ferroelectric nanoparticles: phase field model incorporating strong elastic and dielectric inhomogeneity, Acta Mater. 61 (2013) 7591-7603.

[4] J.J. Wang, Y. Song, X.Q. Ma, L.Q. Chen, C.W. Nan, Static magnetic solution in magnetic composites with arbitrary susceptibility inhomogeneity and anisotropy, J. Appl. Phys. 117 (2015) 043907.

[5] P. Hu, J. Wang, Y. Shen, Y. Guan, Y. Lin and C.W. Nan, Highly enhanced energy density induced by hetero-interface in sandwich-structured polymer nanocomposites, J. Mater. Chem. A 1 (2013) 12321.